On Vortex-induced Oscillation of Bluff Bodies

By

Naruhito SHIRAISHI*, Masaru MATSUMOTO**,
Hideto MASHIMO*** and Akihiro HONDA****

(Received June 30, 1983)

Abstract

This paper considers the classification of vortex-induced oscillations and the geometrical shape effects on them. The following points are considered: 1) the flow pattern around the section, 2) the relation between the onset critical reduced velocity and the critical reduced velocity which is defined as the reciprocal of the Strouhal Number and 3) the relation between the two onset critical reduced velocities of vortex-induced oscillations (in the heaving and the torsional mode). Also, an estimation of "the onset critical reduced velocity" and "the allowable amplitude concerning the fatigue failure of steel" of vortex-induced oscillation is described.

1. Introduction

Today, we can see many long-spanned suspension bridges and cable-stayed bridges, and, still more are to be constructed. For these bridges, it is necessary to consider their aerodynamic stability concerning flutter phenomena and vortex-induced oscillation in detail.

It has been reported that vortex-induced oscillation often occurs with aerodynamically bluff members like the H shape, and with a bluff deck of girder. Generally, vortex-induced oscillation is not so violent nor catastrophic a vibration compared with flutter or galloping. But it might cause trouble with structural fatigue or serviceability because it occurs at a rather low wind speed.

The nature of vortex-induced oscillation remains unknown in spite of many studies. Bridge engineers are so eager to find the aerodynamically stable bridge deck section that they make "trial and error wind tunnel tests" to find a reformed section or effective improvement such as flaps, deflectors, fairings, splitter plates and so on.

This paper considers the classification of vortex-induced oscillations and the

---

    *   Professor, Dept. of Civil Engineering, Kyoto Univ.
   **   Associate Professor, Dept. of Civil Engineering, Kyoto Univ.
 ***   Ministry of Construction
****   Graduate Student, Dept. of Civil Engineering, Kyoto Univ.

geometrical shape effects on them. Aiming at a practical design, it describes how to estimate "the onset critical reduced velocity" and "the allowable amplitude concerning the fatigue failure of steel" of vortex-induced oscillation.

2. Classification of Vortex-Induced Oscillation

This paper classifies vortex-induced oscillation into three types[1] from the following points: 1) the flow pattern around the oscillating section, 2) the relation between the onset critical reduced velocity and the critical reduced velocity which is defined as the reciprocal of the Strouhal Number 3) the relation between the onset critical reduced velocity of heaving and of torsional vortex-induced oscillations.

Namely, they are the "completely separating flow type", the "separating vortex from the leading edge type" and the "attaching flow type".

2.1 Completely Separating Flow Type

A typical example of this type occurs with a fairly bluff section (large ratio of height to width).

The flow is so strongly separated at the leading edge of the section that the whole section is included in the separation region. To see the flow pattern around the heaving section, it can be recognized that the separating flow from the leading edge forms periodical vortices at the trailing edges.

2.2 Separating Vortex From The Leading Edge Type

This type is the most common in the case of bridge deck sections.

The vortex is generated by the leading edge motion, and it flows along the side-surface. The trailing edge motion also generates another kind of vortex. To see the flow pattern around the oscillating section, it can be recognized that "the separating vortex from the leading edge" and "the secondary vortex at the trailing edge" coagulate after the elapse of a natural period and its multiples for the heaving mode. The elapse of half a natural period and a half plus multiples of the natural period for the torsional mode is illustrated in Fig. 1. Assuming that the velocity at which "the separating vortex from the leading edge" flows along the side-surface is proportional to the approaching flow velocity, some relation of the onset critical reduced velocity can be suggested. Namely, the heaving oscillation occurs at Vo and (1/2) Vo while on the other hand, torsional oscillation occurs at 2Vo and (2/3) Vo, in which Vo is the standard onset critical reduced velocity of heaving oscillation, to be explained later.

Therefore, in this type of vortex-induced oscillation, the critical reduced velocity in the heaving mode differs from it in the torsional mode. And these critical reduced velocities seem independent of the Strouhal Number.
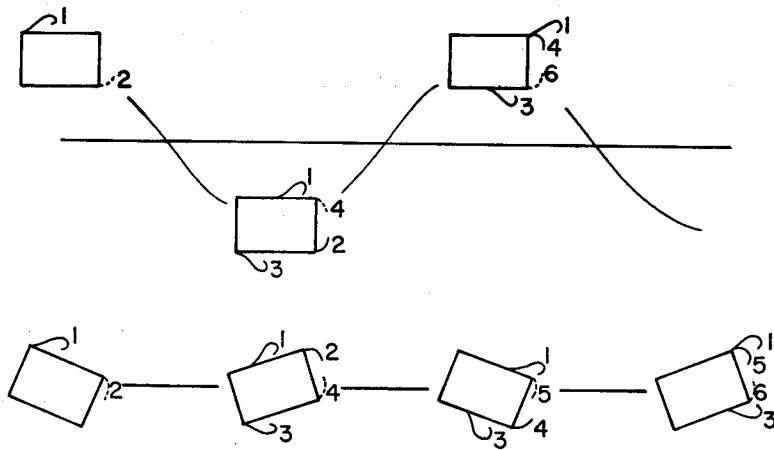
Fig. 1   Separating Vortex From The Loading Edge Type

2.3 Attaching Flow Type

This type occurs when the section is flat.

"The separating vortex from the leading edge" attaches to the side-surface of the oscillating section, and it does not contribute to the oscillation significantly. In the neighborhood of the trailing edge, the secondary wake and "the separated vortex at trailing edge" play an important role in exciting the oscillation.

There is no evident difference in the phase when these two kinds of vortices are generated between heaving and torsional motions, as shown in Fig. 2. Consequently, both heaving and torsional oscillations occur at the same reduced velocity.
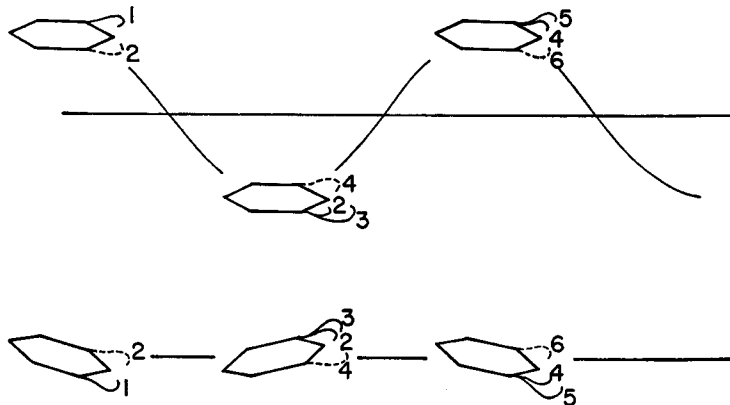

Fig. 2   Attaching Flow Typpe

3. Geometrical Shape Effects on Vortex-Induced Oscillation

3.1 Models and Test Equipments

This chapter takes six models, as shown in Fig. 3. Namely, they are rectangular (model A), trapezoidal (model B), shape Ⅱ (model C), shape Ⅱ (model D), round-edged rectangular (model E) and flat hexagonal (model F).

These models have the same width of 300 mm and the same span length of 930 mm. In order to change the bluffness of the sections, we take three different heights (60, 37.7 and 25 mm) for each section.

The wind tunnel belongs to the Department of Civil Engineering, Kyoto University, and it can generate a two-dimensional uniform flow of the velocity 0-20 m/sec. The working section is 2.5 m wide and 1.5 m high. 8 coil-springs support the model to give it two degrees of freedom (heaving and torsional).

Also, a water flume test was carried out in order to observe the flow pattern around the section. The water flume is 1.0 m wide, 0.4 m deep and 8 m long. To observe the flow pattern we put alumunium-powder into water and moved the model at a constant velocity.

3.2 Geometrical Shape Effects On The Vortex-induced Oscillation

The characteristics of wind tunnel test models are summerized in Table 1. Fig. 4 to Fig. 9 show the Velocity-Amplitude Curve of these models. Instead of deck height (D) and deck width (B), the representative length is the effective deck height ($\bar{D}$) and the effective deck width ($\bar{B}$) as shown in
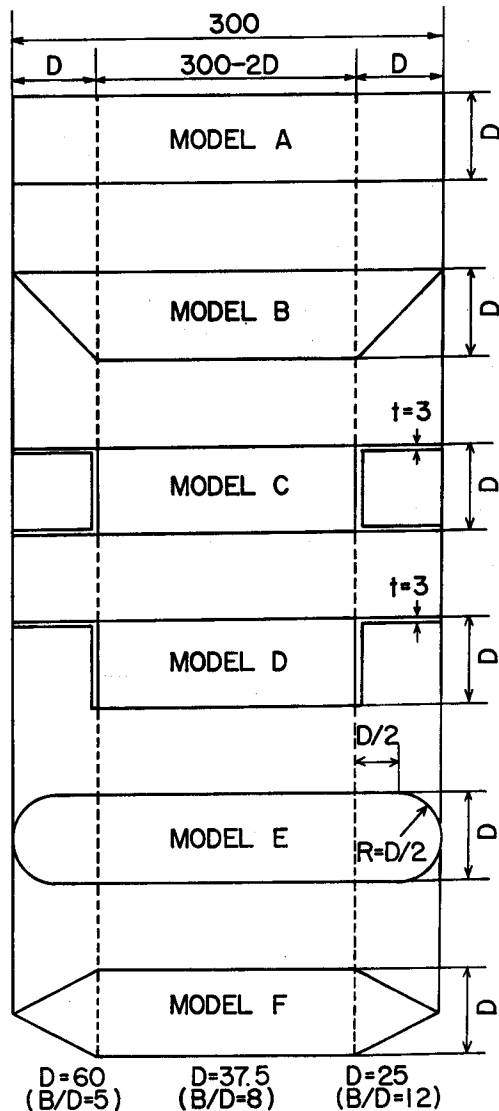

Fig. 3 Cross Sections of Models

Fig. 10. In these figures, the arrow indicates the value which is reciprocal of the Strouhal Number.

Table-1 Characteristics of wind tunnel test models

| Model	α pitching angle	m mass $\left(\dfrac{\text{kg sec}^2}{\text{m}^2}\right)$	I inertia (kg sec²)	f_η deflectional frequency (cps)	f_ϕ torsional frequency (cps)	logarithmic decrement		mass parameter	
						δ_η	δ_ϕ	$\dfrac{m\delta_\eta}{\rho \bar{D}^2}$	$\dfrac{I\delta_\phi}{\rho \bar{D}^4}$
5-A	7	0.3436	0.005733	2.5510	4.8956	0.01368	0.02932	4.07	15.76
5-B	7	0.3901	0.006249	2.5446	4.8544	0.01592	0.02431	6.30	19.54
5-C	7	0.4050	0.005858	2.5615	4.8780	0.01865	0.02634	6.54	14.47
5-D	7	0.3889	0.005719	2.5641	4.8745	0.01665	0.02524	6.57	18.57
5-E	7	0.3843	0.005732	2.5745	4.8611	0.01035	0.02843	4.04	20.97
5-F	7	0.3977	0.005623	2.5706	4.9180	0.01173	0.02613	5.62	26.68
8-A	7	0.3443	0.005593	2.7193	4.9451	0.01675	0.02265	8.48	34.20
8-B	7	0.3330	0.005328	2.7642	5.1056	0.01629	0.02335	9.06	43.38
8-C	7	0.3504	0.005760	2.7230	4.9819	0.01930	0.02068	9.94	32.16
8-D	7	0.3856	0.005482	2.7041	5.0064	0.01919	0.02294	12.36	43.85
8-E	7	0.3395	0.005550	2.7397	5.0118	0.01173	0.02080	6.65	40.25
8-F	7	0.3553	0.005310	2.7806	5.0824	0.01773	0.02085	12.06	50.73
12-A	7	0.3166	0.004853	2.8610	5.2632	0.02505	0.01612	16.85	44.12
12-B	7	0.3367	0.005016	2.8404	5.2301	0.01382	0.01842	10.94	63.85
12-C	7	0.3257	0.005067	2.8281	5.1772	0.01612	0.02105	11.15	60.15
12-D	7	0.3215	0.004942	2.8641	5.2805	0.02474	0.01151	18.70	39.31
12-E	7	0.3620	0.004893	2.8302	5.2542	0.01289	0.02210	10.97	74.73
12-F	7	0.3127	0.004959	2.8495	5.2344	0.02072	0.01888	16.96	80.21
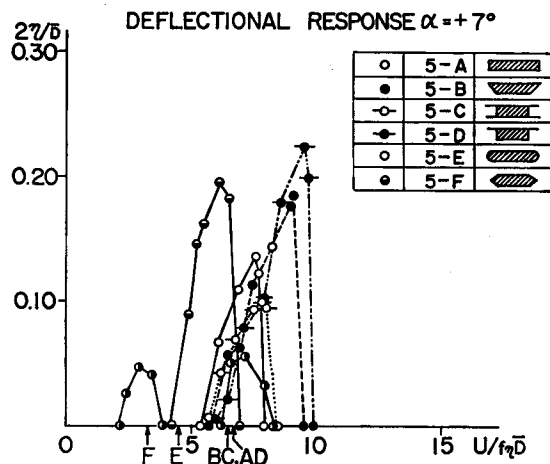
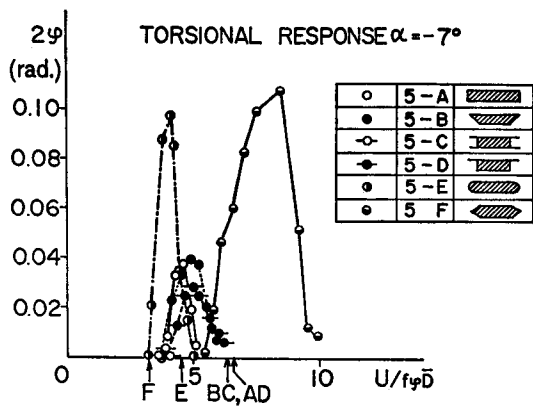Fig. 4 Response Characteristics

Fig. 5　Response Characteristics
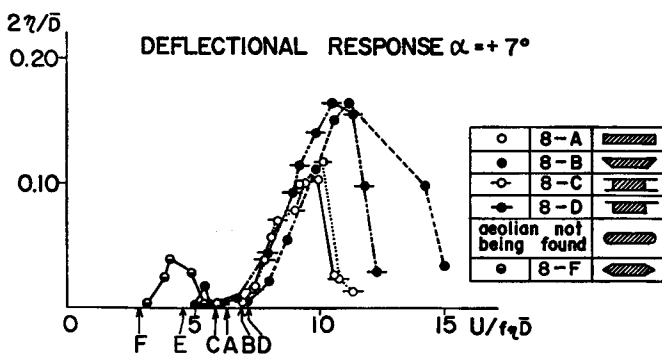
Fig. 6　Response Characteristics

Fig. 7　Response Characteristics

DEFLECTIONAL RESPONSE $\alpha = -7°$

o	12-A	
●	12-B	
-o-	12-C	
-●-	12-D	
aeolian not being found		
aeolian not being found		

Fig. 8   Response Characteristics

TORSIONAL RESPONSE $\alpha = +7°$

o	12-A	
●	12-B	
-o-	12-C	
-●-	12-D	
aeolian not being found		
aeolian not being found		
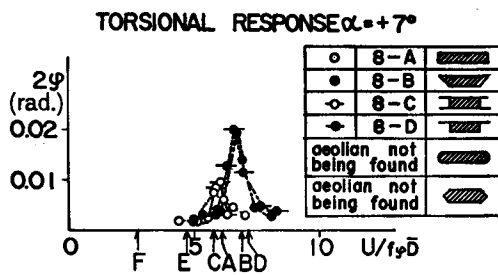
Fig. 9   Response Characteristics
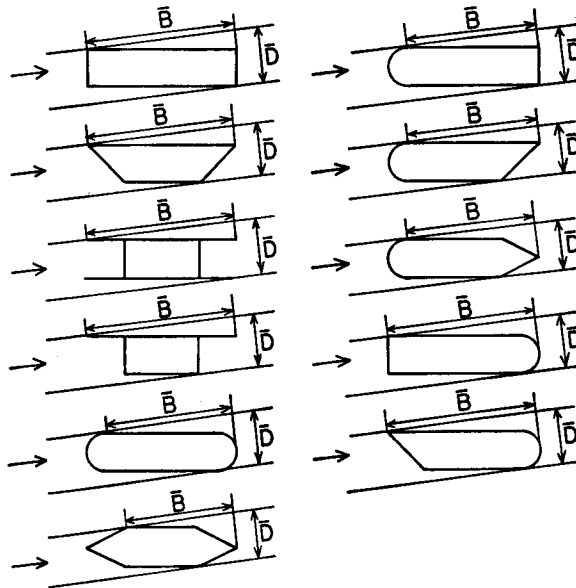
Fig. 10   Effetive Deck Width and Effective Deck Height

Table-2 onest critical reduced velocity

	A	B	C	D	E	F
HEAVING	6	6	6	6	2.5	5
TORSIONAL	4	4	4	4	4	5

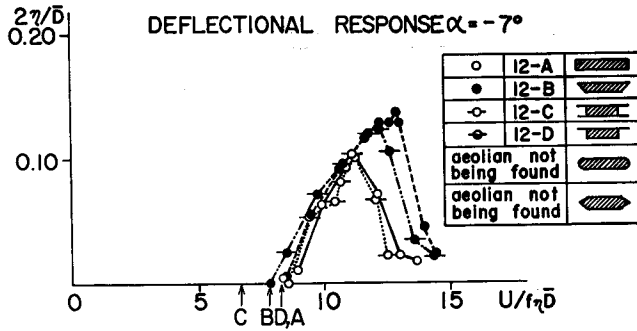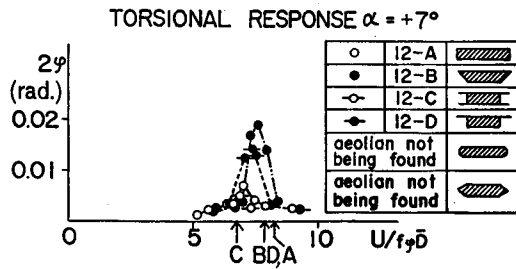At first, the onset critical reduced velocity is studied. Table 2 shows the onset critical reduced velocity in vortex-induced oscilations. This indicates that sections A, B, C and D belong to the "separating vortex from the leading edge type" and section F belongs to the "attaching flow type". Section F is, however, difficult to casslify into any type.

Secondly, the flow patterns around the oscillating sections are considered. The flow patterns are observed when the oscillating amplitude reaches maximum. The flow patterns around sections A, B, C and D are so similar to one another that the flow pattern around section B is compared with the pattern around section F. To see the flow pattern around secton B, the "separating vortex from the leading edge type" displays its characteristics. Namely, the leading edge generates a separating vortex. It flows along the deck until it joins the secondary wake vortex in the neighborhood of the trailing edge. In heaving motion, it takes one period for "the separating vortex from the leading edge" to reach the trailing edge. On the other
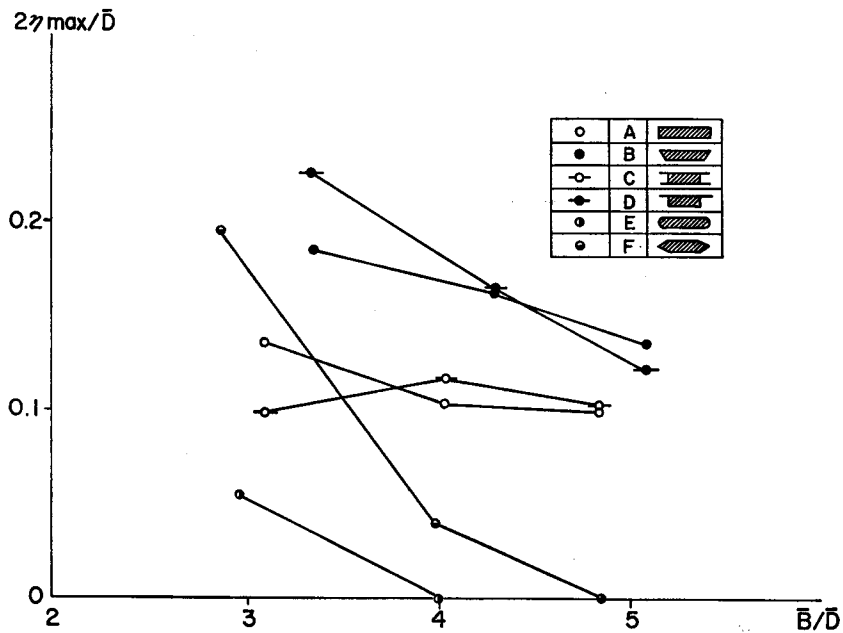

Fig. 11 Reduced Maximum Heaving Amplitude and Slenderness Ratio

hand, it takes one and half periods in torsional motion. To observe the flow pattern around section F, the "separating vortex from the leading edge" can't be found, as the "secondary wake vortex" and the "separating vortex at the trailing edge" seem to have an important function. These flow patterns suggest that the mechanisms of vortex-induced oscillation are different from each other.

Thirdly, it is considered how the onset critical reduced velocity changes according to the slenderness ratio $(\bar{B}/\bar{D})$. Concerning sections A, B, C and D, the onset critical reduced velocity of each section increases as the slenderness ratio increases. If the slenderness ratio is the same, the geometrical shape does not dramatically change the onset critical reduced velocity. On the other hand, the slenderness ratio of section F does not change the onset critical reduced velocity. These relations are explained later.

Lastly, Fig. 11 shows the relation between "the slenderness ratio" and "the reduced maximum heaving amplitude". Generally, the more slender the section, the smaller the reduced maximum heaving amplitude. Sections E and F are especially stable for vortex-induced oscillation if the slenderness ratio is adequte.

4. Onset Critical Reduced Velocity of Bluff Sections

This chapter considers the relation between "the slenderness ratio" and "the onset critical reduced velocity" of bluff sections[2],[3]. This relation was reviewed briefly in Chapter 3. Here, it is investigated including much more data, as shown in Table 3. Fig. 12 shows this relationship, and it indicates that this relationship has some differences according to the type of vortex-induced oscillation.

1) Completely Separating Flow Type: Instead of onset critical reduced velocity, the reduced velocity at which the oscillating amplitude reaches its maximum level is plotted. The approximate function is:

$$V_{cr}=0.845 \, \exp \, (\bar{B}/\bar{D}) +5.755$$
$$\text{for } (\bar{B}/\bar{D}) \leq 1.0 \qquad (1)$$

2) Separating Vortex From The Leading Enge Type: From the definition, the onset critical reduced velocity can be modified as
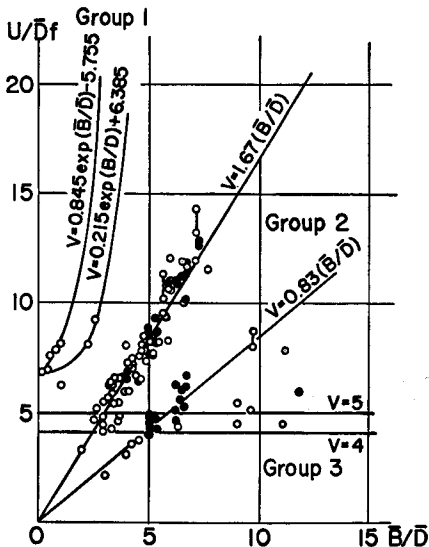

Fig. 12 Reduced Critical Velocity V_{cr1}, V_{cr2} and Slenderness Ratio $\bar{B}/\bar{D}$

Table-3 Cross Sections and Angle of Attack

NO			NO			NO			NO		
1		0°	29		7°	57		0°	85		0°
2		0°	30		0°	58		0°	86		3°
3		0°	31		4°	59		0°	87		3°
4		0°	32		5°	60		0°	88		4°
5		0°	33		7°	61		2°	89		3°
6		4°	34		7°	62		0°	90		4°
7		0°	35		5°	63		0°	91		4°
8		0°	36		7°	64		5°	92		4°
9		10°	37		0°	65		0°	93		3°
10		7°	38		7°	66		7°	94		0°
11		0°	39		7°	67		7°	95		3°
12		10°	40		4°	68		0°	96		3°
13		10°	41		0°	69		5°	97		0°
14		-4°	42		6°	70		0°	98		0°
15		10°	43		5°	71		0°	99		3°
16		-5°	44		3°	72		0°	100		0°
17		10°	45		7°	73		0°	101		0°
18		7°	46		7°	74		0°	102		0°
19		10°	47		0°	75		0°	103		3°
20		5°	48		5°	76		0°	104		-4°
21		.7°	49		5°	77		-4°	105		4°
22		7°	50		7°	78		3°	106		0°
23		0°	51		5°	79		4°	107		4°
24		7°	52		0°	80		3°	108		4°
25		0°	53		7°	81		0°	109		0°
26		7°	54		5.2°	82		3°	110		0°
27		4°	55		4°	83		-3°	111		0°
28		5°	56		7°	84		0°	112		0°

$$V_{cr} = U_{cr}/(\bar{D}f_0) = (U^*/\bar{B}f_0)(U_{cr}/U^*)(\bar{B}/\bar{D}) \tag{2}$$

V_{cr} : onset critical reduced velocity

U_{cr} : onset critical velocity (approaching velocity) (m/sec.)

f_0 : natural frequency (Hz)

U^* : average down flow velocity of separating vortex from the leading edge along the side-surface (m/sec.)

$\bar{D}$: effective deck height (m)

$\bar{B}$: effective deck width (m)

The heaving oscillation of this type occurs when "the separating vortex from the leading edge" reaches the trailing edge in one period of oscillation. So,

$$\bar{B}=U^*T_0=U^*/f_0 \tag{3}$$

From Eq. (1) and (2), we find

$$V_{cr}=(U_{cr}/U^*)\,(\bar{B}/\bar{D}) \tag{4}$$

On the other hand, the unsteady pressure distribution (phase characteristics) suggests that the next equation will anticipate the average down flow velocity from the leading edge:

$$U^*=0.6U_{cr} \tag{5}$$

So, the relation between "the slenderness ratio" and "the onset critical reduced velocity" is obtained:

$$V_{cr}=1.67(\bar{B}/\bar{D}) \tag{6}$$

In the case of torsional oscillation, the next equaton is derived in the same way.

$$V_{cr}=0.83(\bar{B}/\bar{D}) \tag{7}$$

3) Attaching Flow Type: "The slenderness ratio" does not change the onset critical reduced velocity. The relation is estimated

$$V_{cr}=4 \qquad (St=0.25) \tag{8}$$
$$V_{cr}=5 \qquad (St=0.20) \tag{9}$$

5. Allowable Amplitude for Vortex-Induced Oscillation From a Side View of Fatigue

As far as vortex-induced oscillation is concerned, many issues remain, e. g. the mechanism, how to suppress the amplitude and so on. As things stand, we have to permit some amplitude.

In order to design a steel bridge deck, it is necessary to check the safety of the fatigue failure, as shown in Fig. 13[4]. This Chapter considers an allowable amplitude for the vortex-induced oscillation from a side view of the fatigue.

5.1 Wind Velocity Occurrence Rate

It is necessary to know the wind velocity occurrence rate at the place where bridge is to be constructed. Therefore, we should estimate how many times vortex-induced oscillation occurs during the design allowable years.

It is reported[5] that the next Weibull-distrbution will supply the wind velocity occurrence rate characteristics which are observed at 157 observatories in Japan from
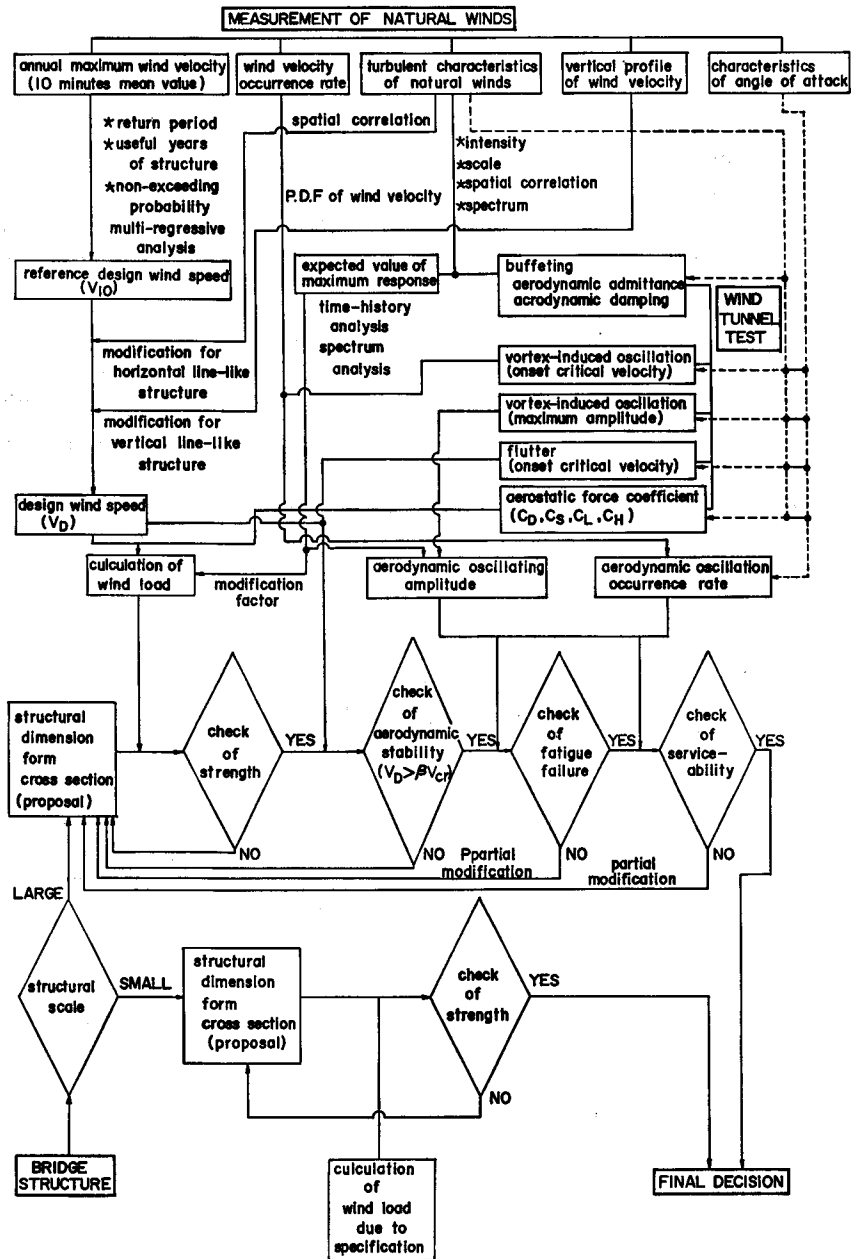
MEASUREMENT OF NATURAL WINDS

| annual maximum wind velocity (10 minutes mean value) | wind velocity occurrence rate | turbulent characteristics of natural winds | vertical profile of wind velocity | characteristics of angle of attack |

★ return period
★ useful years of structure
★ non-exceeding probability
multi-regressive analysis

spatial correlation

P.D.F of wind velocity

★intensity
★scale
★spatial correlation
★spectrum

reference design wind speed (V$_{10}$)

expected value of maximum response

time-history analysis
spectrum analysis

buffeting
aerodynamic admittance
acrodynamic damping

WIND TUNNEL TEST

modification for horizontal line-like structure

modification for vertical line-like structure

vortex-induced oscillation (onset critical velocity)

vortex-induced oscillation (maximum amplitude)

flutter (onset critical velocity)

design wind speed (V$_D$)

aerostatic force coefficient (C$_D$,C$_S$,C$_L$,C$_H$)

calculation of wind load   modification factor

aerodynamic oscillating amplitude

aerodynamic oscillation occurrence rate

structural dimension form cross section (proposal)

check of strength — YES — check of aerodynamic stability (V$_D$>βV$_{cr}$) — YES — check of fatigue failure — YES — check of service-ability — YES

NO   NO Ppartial modification   NO partial modification   NO

LARGE

structural scale — SMALL — structural dimension form cross section (proposal) — check of strength — YES

NO

BRIDGE STRUCTURE

calculation of wind load due to specification

FINAL DECISION

Fig. 13   Designing Procedure concerned with Aerodynamic Instability

1967 to 1977.

Probability density function:

$$f(V) = (k/C)(V/C)^{k-1}\exp(-(V/C)^k) \tag{10}$$

Probability distribution function

$$F(V) = \int_0^V f(V)dV = 1 - \exp(-(V/C)^k) \tag{11}$$

where

> V : wind velocity (m/sec.)
>
> k : shape parameter
>
> C : scale parameter
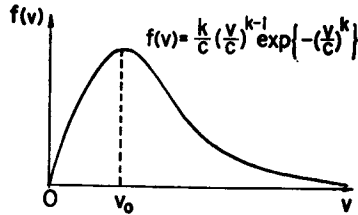
Fig. 14 illustrates the outline of the Weibull-distribution.

Fig. 14   Outline of the Weibul-Distribution

5.2 Allowable Amplitude For Vortex-induced Oscillation

Concerning the fatigue failure of steel, the following equation (12) indicates the relation between the limit amplitude and the repeated number of times.

$$a_i = a_0(\bar{N}/N_i)^\alpha$$

in which

> a_0 : limited amplitude for fatigue failure at repetition number of times $\bar{N}(2 \times 10^6)$
>
> a_i : limited amplitude for fatigue failure at repetition number of time N_i
>
> a_{cr} : first through limited amplitude
>
> α : gradient of $S - N$ Curve

If the Velocity-Amplitude Curve is modeled as in Fig. 15, the allowable amplitude for fatigue failure can be estimated as follows.

At first, the probability vortex-induced oscillation occurs is derived from Eq. (11):

Fig. 15   Model of Velocity-Amplitude Curve

$$p_v = \sum_l p_l p_2(\exp(-V_1/C)^k) - \exp(-(V_2/C)^k))_l \tag{13}$$

in which

> p_l : probability that wind blows from direction l
>
> p_2 : probability that wind blows with the angle of attack at which vortex-induced oscillation occurs
>
> V_1 : velocity at which vortex-induced oscillation occurs
>
> V_2 : velocity at which vortex-induced oscillation expires

Then, the number of times when the vortex-induced oscillation occurs is:
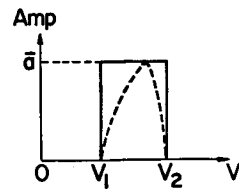
$$N_i = T_0 f_0 p_i \tag{14}$$

in which

N_i : the number of times when vortex-induced oscillation occurs

T_0 : useful years of structure

f_0 : frequency of structure

Substituting Eqs. (13) and (14) into Eq. (12), the allowable amplitude a_i is:

$N_i \geq N_{cr}$

$$a_i = a_0 (2 \times 10^6)^{\alpha} (T_0 f_0 \sum_l p_l p_2 (\exp(-V_1/C)^k) - \exp(-(V_2/C)_k)_l)^{-\alpha}$$

$N_i < N_{cr}$

$$a_i = a_{cr}$$

Now, a case of a specific bridge is investigated in this manner:

useful years (T_0) : 100 years

heaving natural frequency (f_0) : 0. 4 Hz

deck width (B) : 18. 25 m

limit amplitude for fatigue failure at repetition number $\bar{N}$: 0. 2 m

first through limited amplitude (a_{cr}) : 1. 2 m

gradient of S-N Curve (α) : 0. 25

$V_1 = 1. 5 V_2$

probability that wind blows from direction $l(p_i)$: 20%

probability that wind blows with the angle of attack at which vortex-
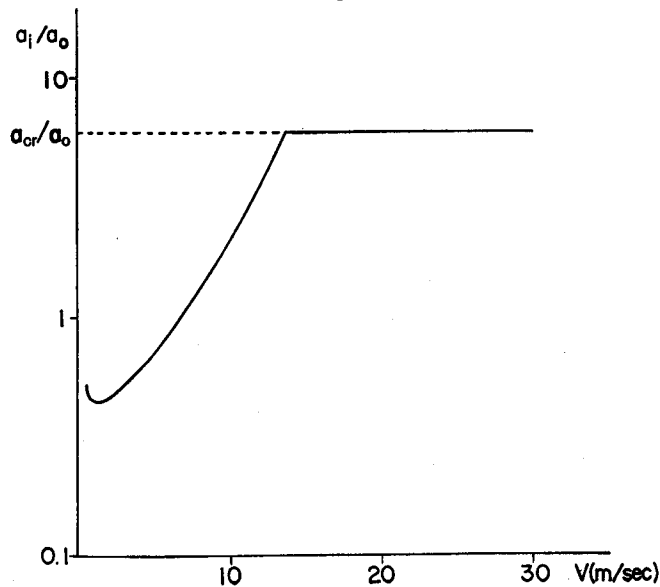induced oscillation occurs (p_2) : 100 %

Fig. 16 Safety Region of the Onset Critical Velocity and Oscillating Amplitude

Weibul-distribution: data of Kyoto $(k=1.25, C=1.89)$

The result is shown in Fig. 16. This shows the safety region of the onset critical velocity and the oscillating amplitude.

6. Conclusion

1) Vortex-induced oscillation can be classified into three general types from the points of response characteristics and the flow pattern around the oscillating section. Namely, they are the "completely separating flow type", the "separating vortex from the leading edge type" and the "attaching flow type".

2) In the "separating vortex from the leading edge type", the onset critical reduced velocity in the heaving mode differs from it in the torsional mode. This indicates that this type is independent of the Strouhal Number. From the flow pattern, the coagulation of the "separating vortex from the leading edge" and the "secondary wake vortex" plays an important part in this type.

3) In the "attaching flow type", the onset critical reduced velocity in both modes (heaving and torsional) are the same. This type is closely related to the Strouhal Number. To see the flow pattern, it is recognized that "the secondary wake vortex" and "the separated vortex at the trailing edge" contribute to this type of oscillation.

4) Concerning the onset critical reduced velocity the ratio of effective deck width to the effective deck height $(\bar{B}/\bar{D})$ seems to be a controlling-factor. This relation depends on the type of vortex-induced oscillation.

5) Maximum oscillating amplitude seems dependent on the configuration, mass parameter and damping of the model.

6) Chapter 5 concerns itself with the safety region of the onset critical reduced velocity and the oscillating amplitude concerning fatigue failure of steel.

Acknowledgements

Reference

1) N. Shiraishi, & M. Matsumoto, On Classification of Vortex-Induced Oscillation and its Application for Bridge Structures, Proc. of the 6th Int'l., Conf. of Wind Engineering, Gold Coast, 1983.
2) Bridge Aerodynamics, Proposed British Design Rules, ICE, London, Jan., 1981.
3) T. A. Wyatt & C. Scruton, A Brief Survey of the Aerodynamic Stability problems of Bridges, Bridge Aerodynamics, ICE, London, Jan., 1981.
4) M. Matsumoto, Design of Structures (Wind Load) Manual of Data Proceeding and Statistical Analysis, Kansai Branch of JSCE, 1982.
5) N. Shiraishi, M. Matsumoto, F. Nagao, H. Mashimo, A. Honda, On The Effect of Geometrical Shapes of Bridge Structures on Vortex-Induced Oscillations and Some Considerations on Allowable Amplitudes of Vibrations, Proc. of the 7th National Symposium on Wind Engineering, 1982.